

On the Origin of Electrochemical Oscillations in the Picric Acid/CTAB Two-Phase System

Véronique Pimienta,[†] Roberto Etchenique,[‡] and Thomas Buhse*

Centro de Investigaciones Químicas, Universidad Autónoma del Estado de Morelos, Av. Universidad N° 1001, Col. Chamilpa, 62210 Cuernavaca, Morelos, México

Received: February 8, 2001

The oscillatory picric acid/CTAB two-phase system—as introduced by Yoshikawa and Matsubara [*J. Am. Chem. Soc.* **1984**, *106*, 4423–4427]—has been revisited. UV–vis spectroscopic studies were presented that provide a clearer and new insight into the possible kinetic mechanism for the oscillatory behavior. It was shown that the key process in the system is the formation of 1:1 ion pairs between picrate and CTA⁺ at the liquid/liquid interface that desorb and move into the organic phase. Kinetic UV–vis experiments also showed that the presence of alcohol—which was essential to observe oscillatory behavior—inhibits the formation of ion pairs. In the course of this process, this inhibition is released presumably due to the transfer of the alcohol from the interface into the organic phase. The corresponding inhibition/acceleration dynamics were observed in a subsystem experiment as S-shaped, autocatalytic-like kinetics with respect to the ion-pair formation. A new mechanism based on Langmuir–Hinshelwood kinetics was proposed that includes the competitive adsorption of CTA⁺, picrate, and the alcohol at the liquid/liquid interface. The release of inhibition, which depends on the concentration of vacant interface sites and which occurs autocatalytically, expresses the key process for the nonlinear behavior. Computer simulations were performed which confirm that the proposed kinetic mechanism is dynamically reasonable.

Introduction

The dynamics of two-phase oil/water/surfactant systems have been subject of increasing research activities for more than three decades. One important reason for this is the wide variety of nonlinear phenomena of chemical origin such as autocatalytic kinetics,¹ kinetic bistability,² spontaneous oscillations,³ and macroscopic wavelike interfacial movements⁴ that have been observed in these systems under different conditions and under varying chemical compositions. Particular interest for these systems arose by discussions that related the observed phenomena to mechanisms of abiotic self-replication, the occurrence of bio-oscillations, and so-called chemomechanical transduction, i.e., the direct and quasi-isothermal transformation of chemical energy stored in a nonequilibrium system into kinetic energy.

In 1978 and 1979, Dupeyrat and Nakache^{5,6} reported on one of the most instructive examples for nonlinear behavior in a two-phase system. The authors found periodic macroscopic movements at the oil/water interface and oscillations of the electrical potential in a simple system composed of an aqueous phase containing a surfactant—hexadecyltrimethylammonium chloride (CTAC) or hexadecyltrimethylammonium bromide (CTAB)—and an organic phase containing 2,4,6-trinitrophenol (picric acid) dissolved in nitrobenzene. The above authors gave an early mechanistic explanation for the nonlinear phenomena that involves the interaction between the negatively charged picrate anions and the positively charged cationic surfactant.

These two species were assumed to form ion pairs at the oil/water interface and to be removed from it by means of a phase-transfer process. The interfacial movement and oscillatory behavior thus were explained to be driven by local variations of the interfacial tension, which is a part of the Marangoni effect.⁷

Later, Yoshikawa and Matsubara^{3a} revisited the above system in a series of experimental studies. Oscillatory behavior was found not only in respect to the electrical potential but also in the pH of the aqueous phase. Both oscillations in electrical potential and in pH appeared to be synchronized where the variation in pH was found in a small range from about pH 3.4 up to 3.5. It was also shown that in the case of stirring, the oscillations became extinct. On the basis of their findings, the authors proposed a mechanism that involves the transport of picrate and of the surfactant to the oil/water interface and the subsequent formation of inverted micelles that suddenly are transferred into the organic phase after the concentration of the surfactant at the interface has reached a critical value. Due to this threshold concentration, a repetitive process of coverage by the surfactant and the picrate followed by collective distraction of inverted micelles into the organic phase was assumed to be the source for the observed periodic behavior.

In subsequent publications,^{8a,b} both authors transferred the experimental scenario from a beaker into a U-shaped glass tube and imposed the picric acid containing organic phase between two aqueous phases, one containing CTAB and alcohol and the other one sucrose. Experiments showed quasiperiodic oscillations in the electrical potential that lasted for several hours. The authors also found that the oscillation frequency increased by increasing the alcohol concentration, and they observed a critical concentration for the alcohol under which no oscillations occurred. This critical concentration was found to decrease by an increase in the hydrophobicity of the alcohols (for example,

* Corresponding author. E-mail: buhse@uaem.mx. Tel: +52 73297997. Fax: +52 73297998.

[†] Permanent address: Laboratoire des IMRCP, UMR au CNRS N° 5623, Université Paul Sabatier, 118 route de Narbonne, 31062 Toulouse Cedex, France.

[‡] Present address: DQIAyQF, Facultad de Ciencias Exactas y Naturales, Pab. 2, Universidad de Buenos Aires, Ciudad Universitaria, CP 1428, Buenos Aires, Argentina.

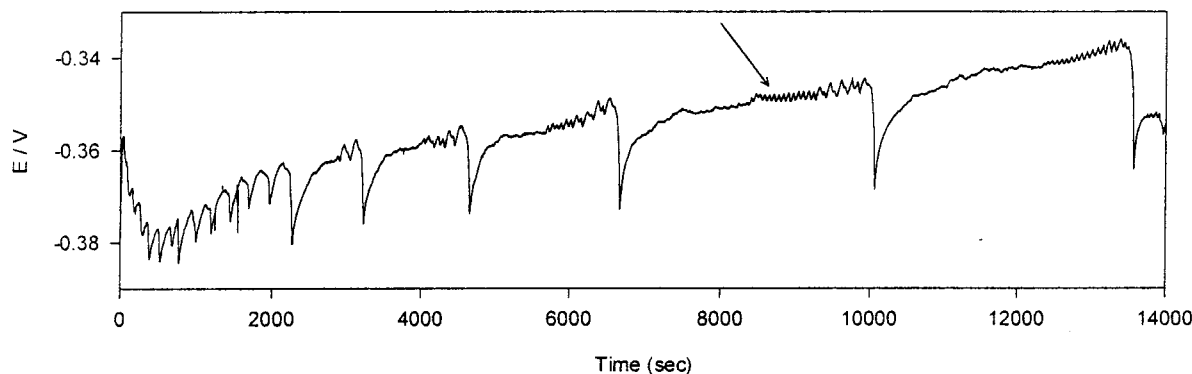


Figure 1. Oscillations of the electrical potential in the picric acid/CTAB two-phase system. The electrical potential was recorded between the two aqueous phases AQ I and AQ II (AQ I = 5 mM CTAB + 0.4 M *n*-butanol, AQ II = 0.1 M sucrose, organic phase = 2.0 mM picric acid in CH_2Cl_2). The arrow indicates the occurrence of an apparently second oscillation pattern located between each of the high-amplitude spikes.

by the use of *n*-pentanol vs ethanol). The mechanistic interpretation of the oscillations remained basically unchanged in respect to the previous one^{3a}—except that, due to the different setup, a transport of CTA^+ across the organic phase into the sugar-containing aqueous phase was suggested.

Later Toko et al.^{3g} proposed a different interpretation for the oscillatory behavior in electrical potential and in pH on the basis of the autocatalytic (cooperative) formation of a tightly packed monolayer of ion pairs at the liquid–liquid interface and their subsequent release into the organic phase. However, in their theoretical model, the authors did not take into account the presence of alcohol, which was essential to observe oscillatory behavior in experiment.

In further experimental studies,^{4d} periodic variations of the interfacial tension in similar two-phase systems have been observed. Also, measurements of the molecular number density of the picric acid/CTAB system at the oil/water interface by quasielastic laser scattering were reported⁹ to show periodic behavior. These later findings support the central idea that the oscillations are strongly associated with periodic changes in the interfacial structure between the organic and aqueous phase.

In this work, we revisited the experiment in the glass U-tube. The aims of our study were to clarify the mechanism of the oscillatory dynamics and to give a molecular interpretation of the interfacial cooperative process that is still at a stage of predominantly qualitative assumptions. We will present the results of UV–vis spectroscopic studies that ascertain the formation of ion pairs at the liquid–liquid interface and that also reveal an unexpected influence of the alcohol on the kinetics of this formation. On the basis of these experimental findings, we shall provide new insight into the cooperativity of the system in which the essential nonlinearity stems from a release of inhibition due to the presence of alcohol at the liquid–liquid interface. On the basis of these observations, a tentative kinetic model will be presented in which the alcohol acts as an inhibitor and that gives rise to oscillatory dynamics.

Experimental Section

All chemicals used were of analytical grade. Prior to the experiments, picric acid (Aldrich, A.C.S.) was desiccated under vacuum, and CH_2Cl_2 (Aldrich, HPLC grade) was dried over CaSO_4 . Hexadecyltrimethylammonium bromide, CTAB, (Aldrich, $\geq 99\%$), sucrose (Aldrich, A.C.S.), ethanol (Merck, p.a.), and *n*-butanol (Baker, analyzed) were used as purchased. The water was double-distilled.

Oscillations of the electrical potential were recorded in a vacuum-dried U-shaped glass tube of 8 mm diameter at $25 \pm$

2°C without stirring. The measurement device consisted of two Ag/AgCl electrodes that were placed into the two aqueous phases located on both sides of the U-tube. Alternatively, the electrical potential between one of the aqueous phases and the organic phase was measured by using an electrode equipped with a capillary salt bridge containing a concentrated aqueous solution of KCl. The capillary was then placed across one of the aqueous phase. Prior to each use, the glass apparatus was cleaned with an aqueous solution of ethanol/KOH and then rinsed with water, acetone, and ethanol. The organic solution (4 mL) of CH_2Cl_2 containing 2.0 mM picric acid was placed in the bottom of the U-tube. Then the two aqueous solutions (3 mL each)—one containing 5 mM CTAB and 0.4 M *n*-butanol and the other one containing 0.1 M sucrose—were carefully and simultaneously introduced into the two arms of the tube. After filling, the recording of the electrical potential was started.

The UV–vis spectra were recorded with a HP 8453 diode array spectrophotometer. Solutions coming from 10 times concentrated stock solutions were directly weighed in the quartz cuvettes of 1 cm optical path length. All experiments were performed in a thermostated cell holder at 25°C . Stirring was employed by a Teflon-coated magnetic bar placed at the bottom of the cuvette.

Computer simulations and fitting procedures of UV–vis data have been performed with Sa (version 2.0)¹⁰ on a Pentium III personal computer. The general algorithm used for the numerical integration of the differential equations is based on a semi-implicit Runge–Kutta method.¹¹

Results

Experiments in the U-Shaped Glass Reactor. Figure 1 shows the typical result of an experiment performed in the U-shaped glass reactor after the organic phase (ORG)—containing CH_2Cl_2 (ref 12) and picric acid—has been simultaneously overlaid on one side with aqueous CTAB and butanol (AQ I) and on the other side with an aqueous solution of sucrose (AQ II). The oscillations started after about 2 min, at the beginning with increasing amplitude, and lasted for more than 4 h.

The characteristic spike pattern of the oscillations, describing a steep drop in the potential followed by a slower increase, is in good agreement with the previous findings of Yoshikawa and Matsubara.⁸ As indicated by the arrow in Figure 1, we additionally observed an apparently second oscillation pattern located between each high-amplitude spiking. This oscillation pattern, which is characterized by a high frequency and low amplitude, gives indication for mixed-mode oscillations in this system. We did not observe this phenomenon when *n*-butanol in AQ I was replaced by ethanol.

Almost immediately after introducing both aqueous phases into the reactor, we observed the onset of a deep yellow color formation in the vicinity of ORG/AQ I interface.

Throughout the total time in which we detected the oscillations (i.e., for more than 4 h), AQ I remained transparent and colorless. In contrast to this, yellow color built up slowly in ORG below AQ I and faded out along the tube so that the organic phase about 2 cm below AQ II remained colorless for more than 4 h. In AQ II, we noticed yellow color formation almost instantly after the two phases were in contact.

During about the first 5 min of the experiments—after AQ I respectively AQ II came in contact with ORG—we observed with our eyes periodic wavelike movements of high activity at the AQ I/ORG interface on one side of the U-tube. It appeared that these macroscopic movements were not directly related to the oscillations of the electrical potential since they were out-of-phase, their frequency was significantly higher and their total—eye-visible—lifetime was much shorter than those of the measured oscillations.

In our typical experiments, we measured the electrical potential between AQ I (CTAB and alcohol containing) and AQ II (sucrose containing) as Yoshikawa and Matsubara⁸ did. However, in 1990, Arai et al.¹³ found that the oscillations between AQ I and AQ II can be simultaneously detected by measuring the electrical potential between AQ II and ORG. In contrast to that, the authors did not detect any periodic changes in the electrical potential between AQ I and ORG. In other words: Oscillations occurred exclusively between the organic phase and the sucrose containing aqueous phase. This surprising result was discussed to stand in contradiction with the former mechanistic explanations of Yoshikawa and Matsubara,^{8b} who addressed the oscillatory behavior to the interface between AQ I (CTAB and alcohol containing) and the organic phase. We also measured the potential between AQ I/ORG, AQ II/ORG, and as a reference between the two aqueous phases. Our results were not in agreement with those reported by Arai et al.¹³ We found that the recorded oscillations between AQ I and AQ II are the same as those simultaneously recorded between AQ I and ORG, and—in contrast to the above authors—we did not detect any oscillations by measuring the potential between ORG and the sucrose-containing aqueous phase.

UV–Vis Experiments

Picric acid ($pK_a = 0.38$)—when in contact with water—dissociates to form the yellow colored picrate anion. Figure 2 shows the absorption spectrum of picrate in pure water (c: $\lambda_{max} = 356$ nm) and of picric acid in CH_2Cl_2 (a: $\lambda_{max} = 336$ nm).

Spectrum b in Figure 2 represents picrate in water plus CTAB ($\lambda_{max} = 354$ nm), in which the concentration of CTAB was close to its critical micelle concentration of about 9×10^{-4} M (ref 14). In this case, we observed a shoulder in the spectrum at $\lambda = 415$ nm that completely disappeared when the concentration of CTAB was less than 0.5×10^{-4} M; i.e., the spectrum of picrate became in the later case the same as that in pure water.

Spectrum d in Figure 2 was recorded at equilibrium in a two-phase system under slight stirring in which the organic and aqueous phases remained entirely separated. The light beam was passed through the organic phase (2 mL) of CH_2Cl_2 containing picric acid and CTAB. The organic phase—located at the bottom part of the cuvette—was carefully overlaid with 0.5 mL of pure water. The stirring ensured quasihomogeneous conditions in the organic phase. In this case, we observed a shift of λ_{max} to 370 nm and again a shoulder appeared in the spectrum at about

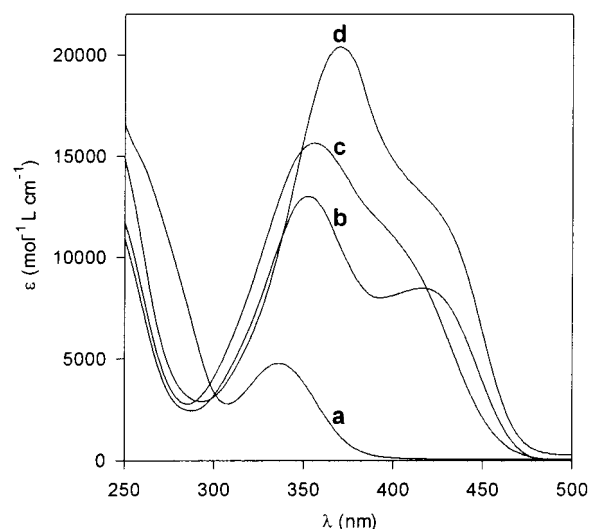
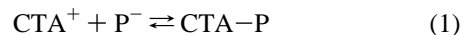


Figure 2. Equilibrium absorption spectra (a) of picric acid in pure CH_2Cl_2 , (b) of picrate in water in the presence of CTAB, (c) of picrate in pure water, and (d) of the organic phase of a two-phase system consisting of $CH_2Cl_2 + 1.0 \times 10^{-4}$ M picric acid + 1.0×10^{-4} M CTAB and of pure water. The values of ϵ were obtained from the Job diagram shown in Figure 3.

$\lambda = 415$ nm. This indicates an interaction between the picrate anion and CTA^+ in the organic phase that only takes place if water is present (note that CTA^+ itself does not show any absorbance at these wavelengths). We suppose that the interaction between CTAB and picric acid takes place at the organic/aqueous interface, which explains that water is essential in this system to assist the dissociation of the two compounds.

To gain closer insight in this question, we recorded a Job diagram¹⁵ by varying the mole fraction (χ) of picric acid in the organic phase in the presence of $(1 - \chi)$ CTAB and measuring the corresponding absorbance of the presumed CTA^+ –picrate complex. These experiments were performed with equally concentrated stock solutions of CTAB and picric acid in CH_2Cl_2 and by weighing various aliquots of the two solutions at a constant combined volume of 2 mL directly into the quartz cuvettes. The general setup (two-phase conditions) was the same as that for spectrum d in Figure 2, and the absorbencies were recorded at equilibrium.

In the case of ion pairs (1:1 stoichiometry)



we would expect a peak value for the absorbance of $CTA-P$ for the case $\chi = 0.5$, where P^- stands for the picrate anion and $CTA-P$ for the 1:1 ion-pair complex.

Figure 3 represents the continuous-variation plot of the CTA^+ /picrate system that shows a maximum in absorbance at $\chi = 0.5$. This clearly indicates the formation of a 1:1 complex. For the cases when $\chi < 0.5$, i.e., $[CTAB] > [picric\ acid]$, the aqueous phase remained colorless and a plane meniscus at equilibrium,¹⁶ indicated the accumulation of CTA^+ at the organic/aqueous interface. For $\chi = 0.5$, the aqueous phase remained colorless, and at the end, the meniscus was curved, which is a sign for the absence of free CTA^+ as well as an indication for the poor performance of the hydrophobic ion pairs to act as an surface-active agent.

Finally, for $\chi > 0.5$, we observed a curved meniscus at equilibrium—once again indicating the complexation of all CTA^+ by picrate—and a yellow colored aqueous phase due to the accumulation of free excess picrate in the water phase. That

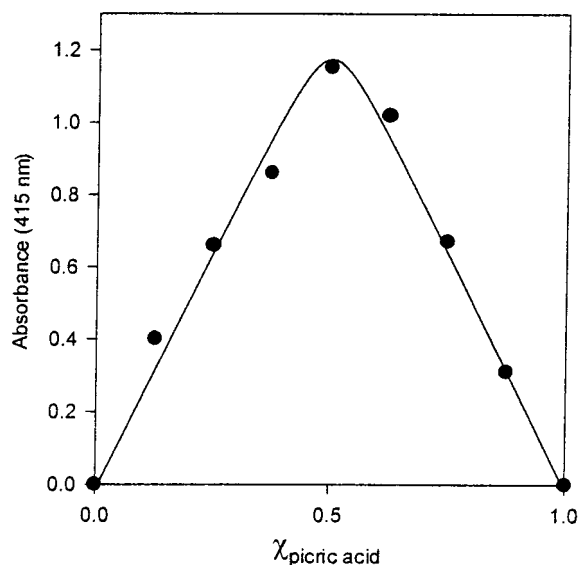


Figure 3. Equimolar Job diagram of the CTAB/picric acid system in CH_2Cl_2 recorded under two-phase conditions at equilibrium (see text for details). At 415 nm, the molar extinction coefficients of picric acid and of CTAB/ CTA^+ in CH_2Cl_2 are negligible. Concentrations of stock solutions $[\text{C}] = 1.0 \times 10^{-4}$ M. Dots, experimental data; continuous line, numerical fitting of experimental data in order to obtain K_{eq} and $\epsilon_{\text{CTA-P}}$.

gives evidence that, under two-phase conditions, picrate quantitatively moves from the organic to the aqueous phase if there is no complexation agent like CTA^+ available.

The continuous line shown in Figure 3 gives the result of a numerical two-parameter fitting based on a method by Micheau and co-workers.¹⁷ This allowed us to estimate the constant for the equilibrium of (1) as $K_{\text{eq}} = 9.0 \times 10^5$ and to find an approximate value for the molar extinction coefficient of $\epsilon_{\text{CTA-P}} = 13200 \text{ mol}^{-1} \text{ L cm}^{-1}$ ($\lambda = 415 \text{ nm}$).

The above-mentioned UV-vis studies strongly indicate a 1:1 complex formation between CTA^+ and picrate. Although the job diagram does not exclude the possibility that ion pairs undergo aggregation in the organic phase, it is interesting to note that the spectrum remained unchanged when we recorded it in the presence of 0.4 M *n*-butanol that was added to the aqueous phase. It was reported¹⁸ for a similar system that the presence of alcohol is essential for CTA^+ to form reverse micelles, but our UV experiments indicate that alcohol was not involved in the interaction of the two compounds under equilibrium.

Furthermore, the possible formation of reverse micelles, which has been proposed in earlier works^{3a, 3b} as a key process for the oscillatory behavior, has been virtually excluded by complementary near infrared measurements. These experiments were based on the capacity of reverse micelles to solubilize water in their hydrophilic cores.¹⁸ Basically, solubilization leads to a broad IR band corresponding to water that is bound to the surfactant (at $\sim 5100 \text{ cm}^{-1}$) and to an increase in the sharp band attributed to free excess water in the organic phase (at 5270 cm^{-1}). We examined the NIR spectrum of a CH_2Cl_2 solution containing CTA-P under the conditions of the original U-tube experiment. We did not detect any of the two effects in reference to the NIR spectrum of a CH_2Cl_2 solution saturated with water and in the presence of 0.4 M *n*-butanol. Although these measurements do not exclude the possible formation of very small and "dry" aggregates, it questions the former assumption^{3a, 3b} of aggregate formation as the impetus for the oscillatory dynamics. Small-sized aggregates, if present at all, can hardly

play the role in the highly cooperative dynamics that will lead to the observed oscillations.

Our investigations were then directed to test the possible effect of alcohol on the kinetics of the ion-pair formation by time-resolved UV-vis experiments. Again, these experiments were performed directly in the quartz cuvette under slight stirring and under two-phase conditions. The initial concentrations of the compounds and the composition of the organic and the aqueous phase were the same as those in the U-tube experiment: organic phase, CH_2Cl_2 + picric acid; aqueous phase, CTAB + *n*-butanol. Because of high concentrations, the absorbance versus time in the organic phase was measured at $\lambda = 460 \text{ nm}$ —instead of the previous $\lambda = 415 \text{ nm}$ —in order to record the time evolution of $[\text{CTA-P}]$. In a control experiment without *n*-butanol, we found approximately first-order kinetics for the formation of CTA-P. In the presence of *n*-butanol, however, the kinetic curve was S-shaped. The same observation was made when *n*-butanol was replaced by ethanol.

To obtain more systematic results for the influence of alcohol, we used less concentrated solutions and started the experiment with picric acid and CTAB in the organic phase and by varying the concentration of *n*-butanol in the aqueous phase. Figure 4A shows the result of one of these experiments in a time-resolved absorbance versus wavelength plot indicating the appearance of an isosbestic point at $\lambda = 305 \text{ nm}$. This gives evidence for the formation of only one product (CTA-P) that is formed by complexation of CTA^+ and picrate.

In Figure 4B, the respective kinetic curves for different initial concentrations of *n*-butanol between 0.2 and 0.5 M at $\lambda = 415 \text{ nm}$ are given. In the absence of *n*-butanol (curve 1), we observed again approximately first-order kinetics for the CTA-P formation. In the presence of the alcohol (curves 2–4), unusual S-shaped kinetic curves were recorded. These show an increase in the induction period when the initial concentration of the alcohol increases. We tentatively interpreted this sigmoidal shape by an inhibitory effect of the alcohol that diminishes in the course of CTA-P formation. The effect appears to be directly correlated to the initial concentration of *n*-butanol.

In the course of the above UV-Vis experiments, we were able to record the spectra of all presumed key species of the system. In the following, we analyzed samples of the oscillatory reaction mixture in the glass U-tube after 4 h, i.e., after the oscillations had diminished. We wanted to identify—in qualitative terms—where these species were located (in AQ I, AQ II, or ORG). The following results were obtained: No picrate was detected in AQ I. In ORG close to AQ I, we recorded a spectrum like that shown in spectrum d of Figure 2, indicating the presence of CTA-P. In ORG close to AQ II, we recorded the typical spectrum of picric acid in CH_2Cl_2 without the presence of CTAB (Figure 2, curve a). In AQ II, we found the spectrum of picrate in water (Figure 2, curve b) but no sign for CTA^+ .

Discussion

Kinetic Mechanism. The first part of our discussion will focus on the clues we can draw from our experimental results in order to suggest a possible mechanism for the oscillatory picric acid/CTAB two-phase system that is based on chemical reasoning. In the second part of the discussion, we will present an attempt to verify the proposed mechanism from the dynamical point of view by suggesting a tentative kinetic model.

It follows directly from experimental evidence that exclusively processes at the interface between AQ I (CTAB and *n*-butanol in water) and ORG (picric acid in CH_2Cl_2) can be considered

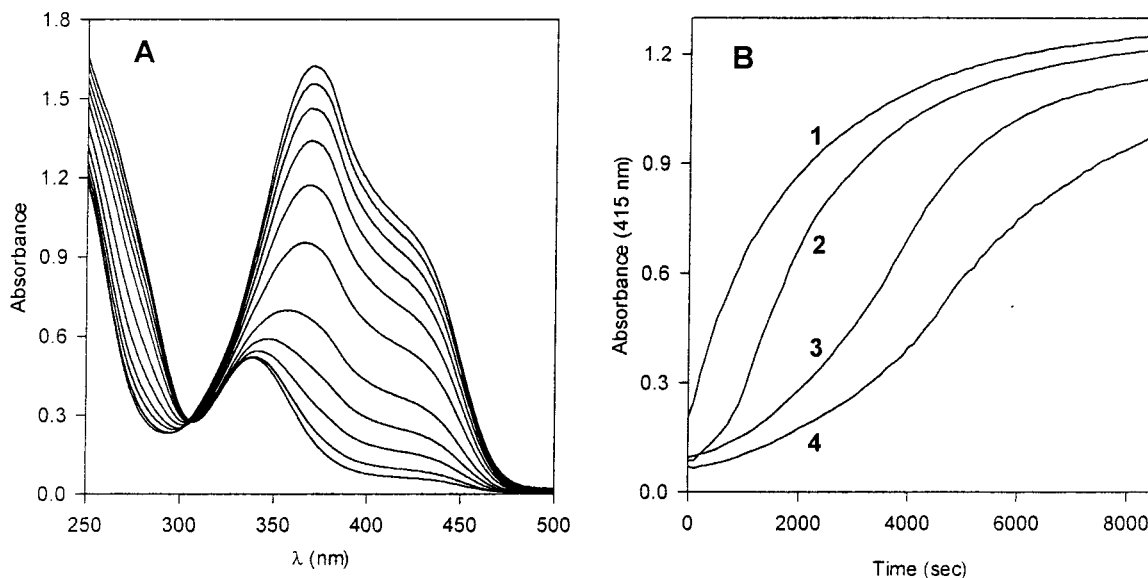
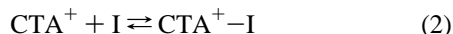


Figure 4. (A) Time-resolved absorption spectra of the CTAB/picric acid system in CH_2Cl_2 in the presence of 0.5 M *n*-butanol recorded under two-phase conditions $[\text{CTAB}]_0 = 1.0 \times 10^{-4}$ M and $[\text{picric acid}]_0 = 1.0 \times 10^{-4}$ M. The spectra were recorded for 10000 s in time intervals of 1000 s. (B) Absorbance vs time plot for a system like that in panel A recorded at 415 nm. Initial concentrations of *n*-butanol are (1) none, (2) 0.2 M, (3) 0.4 M, and (4) 0.5 M.

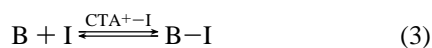
as kinetically active in the sense that they control the oscillatory dynamics of the system.

From the UV-vis batch experiments, we were able to trace the probable origin for the oscillatory dynamics in the system. Namely, this is the inhibitory effect of the alcohol that diminishes during the formation of $\text{CTA}-\text{P}$ ion pairs and that consequently generates S-shaped, autocatalytic-like kinetics under batch conditions. This effect can be interpreted as follows:

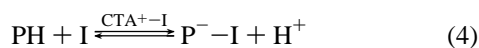
I. After AQ I (CTAB and *n*-butanol containing) and ORG (picric acid containing) get in contact, the AQ I/ORG interface will be covered fast by CTA^+ ions forming a surfactant monolayer. In our mechanism, we express this process in terms of Langmuir-Hinshelwood kinetics as the adsorption of CTA^+ at free sites (I) of the AQ I/ORG interface:



II. Process I is accompanied by a second process in which *n*-butanol (B) moves from AQ I toward the AQ I/ORG interface (note that in a typical experiment B is 80 times more concentrated than CTAB). It was reported²⁰ that alcohol molecules tend to intercalate between surfactant molecules that are adsorbed at water/oil interfaces. Considering a similar effect for B, we have to take into account the intercalation of B between CTA^+-I , which is expressed by step 3 as the adsorption of B at vacant sites of the interface forming B-I. We assume that the rate of this step depends on the concentration of CTA^+-I that is already present. For the kinetic mechanism, we consider that the adsorbed surfactant at the interface acts as a catalyst for the adsorption of *n*-butanol:



III. Steps 2 and 3 proceed simultaneously with a third process when picric acid (PH) coming from ORG arrives at the interface. When coming in contact with water, it rapidly dissociates to form picrate (P^-) and H^+ :



P^- will get trapped at the interface due to the interaction with

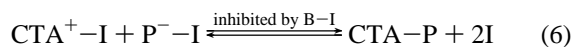
the positively charged CTA^+ and consequently does not reach AQ I. This is supported by our observation that we did not detect any P^- in AQ I. Also, for this process, we considered the assistance of CTA^+-I due to the attraction between the negatively charged picrate and the positively charged surfactant adsorbed at the interface. Thus, we regarded step 4 to be catalyzed by CTA^+-I .

In summary, steps 2-4 can be regarded as a competition between P^- , CTA^+ , and B for free sites at the AQ I/ORG interface. In terms of adsorption kinetics, the total concentration of interface sites $[\text{I}]_0$, occupied or unoccupied, will remain constant, where

$$[\text{I}]_0 = [\text{I}] + [\text{P}^--\text{I}] + [\text{CTA}^+-\text{I}] + [\text{B}-\text{I}] = \text{constant} \quad (5)$$

In the framework of our mechanism, this assumption is fairly reasonable since the surface area of the AQ I/ORG interface remains approximately constant throughout the experiment.

IV. As indicated by our UV-vis experiments, CTA^+-I and P^--I at the interface interact with each other to form the hydrophobic $\text{CTA}-\text{P}$ ion pairs that desorb and move into ORG:



Step 6 has been observed in our UV-vis experiments to be inhibited by *n*-butanol. A possible reason could be that the intercalation of B between CTA^+-I blocks to a certain extent the interaction between CTA^+-I and P^--I and consequently slows down the $\text{CTA}-\text{P}$ formation.

V. One possible pathway for B coming from the aqueous phase was expressed by its intercalation between CTA^+ at the interface and its formation of B-I (step 3) that inhibits the formation of $\text{CTA}-\text{P}$. This step was assumed to be catalyzed by CTA^+-I . On the other hand, the formation of $\text{CTA}-\text{P}$ (step 6) liberates the interface and weakens the interaction between CTA^+ and the alcohol molecules at the interface. In other words, the alcohol can no longer effectively intercalate between CTA^+-I . Regarding now this case in which the interface is mostly unoccupied, which means that $[\text{CTA}^+-\text{I}]$ and $[\text{P}^--\text{I}]$ are low and $[\text{I}]$ is high, B arriving at the interface is considered

TABLE 1: Kinetic Model, Rate Equations, and Differential Equations Used for Simulations of the Oscillatory Picric Acid/CTAB Two-Phase System^a

$\text{CTA}^+ + \text{I} \rightarrow \text{CTA}^+-\text{I}$	$R_1 = k_1[\text{CTA}^+][\text{I}]$	(M1)
$\text{B} + \text{I} \xrightarrow{\text{CTA}^+-\text{I}} \text{B}-\text{I}$	$R_2 = k_2[\text{B}][\text{I}][\text{CTA}^+-\text{I}]$	(M2)
$\text{PH} + \text{I} \xrightarrow{\text{CTA}^+-\text{I}} \text{P}^--\text{I} + \text{H}^+$	$R_3 = k_3[\text{PH}][\text{I}][\text{CTA}^+-\text{I}]$	(M3)
$\text{CTA}^+-\text{I} + \text{P}^--\text{I} \rightarrow \text{CTA}-\text{P} + 2 \text{I}$	$R_4 = (k_4/([\text{B}-\text{I}] + 1))[\text{CTA}^+-\text{I}][\text{P}^--\text{I}]$	(M4)
$\text{B}-\text{I} \xrightarrow{\text{I}} \text{B}' + \text{I}$	$R_5 = k_5[\text{B}-\text{I}][\text{I}]$	(M5)

^a (For the sake of simplicity, reverse reactions have not been taken into account.) Differential equations:

$$\frac{d[\text{CTA}^+]}{dt} = -R_1 + k_f([\text{CTA}^+]_0 - [\text{CTA}^+])$$

$$\frac{d[\text{B}]}{dt} = -R_2 + k_f([\text{B}]_0 - [\text{B}])$$

$$\frac{d[\text{PH}]}{dt} = -R_3 + k_f([\text{PH}]_0 - [\text{P}])$$

$$\frac{d[\text{CTA}^+-\text{I}]}{dt} = R_1 - R_4$$

$$\frac{d[\text{B}-\text{I}]}{dt} = R_2 - R_5$$

$$\frac{d[\text{P}^--\text{I}]}{dt} = R_3 - R_4$$

$$\frac{d[\text{CTA}-\text{P}]}{dt} = R_4 - k_f[\text{CTA}-\text{P}]$$

$$\frac{d[\text{B}']}{dt} = R_5 - k_f[\text{B}']$$

$$\frac{d[\text{I}]}{dt} = -R_1 - R_2 - R_3 + 2R_4 + R_5$$

$$\frac{d[\text{H}^+]}{dt} = R_3 - k_f[\text{H}^+]$$

to travel through the interface directly into ORG. In the mechanism, this is summarized by the following step:



where B' stands for *n*-butanol in the organic phase. This process is in fact autocatalytic with respect to I and it becomes increasingly effective when the concentration of free interface sites increases. Note also that steps 3 and 7 are linked by means of relation 5.

Taking into account processes I–V, the sigmoidal shape in the kinetic curve of CTA–P formation can be understood as a release of the inhibition in step 6. The formation of ion pairs generates vacant interface sites and accelerates the desorption of the inhibitor (B–I): the dynamics of inhibition and its autocatalytic release are crossed linked through the concentration of I.

Following our results, the only process occurring at the AQ II (sucrose in water)/ORG interface on the other side of the reactor is the conversion of PH into picrate P[−] at the interface and the slow accumulation of P[−] in the aqueous phase. Thus, for the AQ II/ORG interface, the only process would be



Since we did not detect any oscillations across the AQ II/ORG interface, process 8 seemingly does not interfere with the kinetics at the AQ I/ORG interface. In fact, the role of added

sucrose to AQ II has yet to be fully understood, and no explanation for its use has been given so far. In control experiments, without adding sucrose to AQ II, we also observed oscillatory behavior, but with an increase in the signal noise and with smaller amplitude in respect to those where sugar has been added. On the other hand, and within experimental accuracy, side experiments showed that the presence or absence of sucrose did not affect the diffusion coefficient or the partition coefficient of picrate that diffuses into AQ II. Furthermore, the estimated bulk viscosity of AQ II after addition of sucrose is about 1.1 mPa s, which is still very close to that of pure water and cannot explain the change in the signal noise and amplitude. However, it is possible that the microviscosity in the vicinity of the liquid/liquid interface shows a considerably higher value. For this case, a tentative explanation for the role of sucrose could be given by a change in the interfacial properties between AQ II and ORG that could result in the observed dampening of the small-scale oscillations. In any case, we have shown by our experiments that no oscillations occur at the interface between AQ II and ORG but exclusively between AQ I and ORG. We take this as an indication that the presence of sucrose probably does not affect the oscillatory dynamics but rather dampens the recording of the signal.

Modeling and Computations

In the following, we will translate the above reasoning into a numerical model in order to test if the dynamics of the proposed mechanism can indeed generate oscillatory behavior.

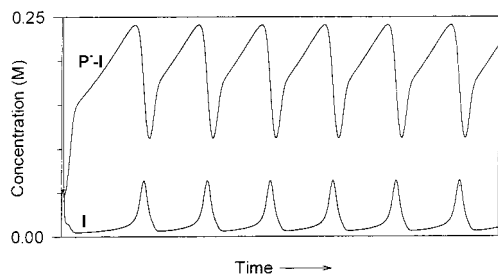


Figure 5. Numerical simulation of oscillatory behavior in the CTAB/picric acid system on basis of the kinetic model (Table 1) to which flow terms have been added (see text for details). Kinetic parameters: $k_1 = 0.5 \text{ M}^{-1} \text{ s}^{-1}$, $k_2 = 0.01 \text{ M}^{-2} \text{ s}^{-1}$, $k_3 = 60 \text{ M}^{-2} \text{ s}^{-1}$, $k_4 = 0.0225 \text{ M}^{-1} \text{ s}^{-1}$, $k_5 = 0.0005 \text{ M}^{-1} \text{ s}^{-1}$. Flow rate constant: $k_f = 0.01 \text{ s}^{-1}$; $[I]_0 = 1.0 \text{ M}$. Inflow concentrations: $[B]_0 = 1.0 \text{ M}$, $[CTA^+]_0 = 0.015 \text{ M}$, $[PH]_0 = 0.01 \text{ M}$.

For this reason, we have made additional assumptions. First, the model only takes into account the processes taking place at the interface between AQ I (CTA^+ and alcohol containing) and ORG. Second, we simulated in a simplified fashion the diffusive flux of B, CTA^+ , and PH by means of an open-flow system in which these species enter the system, i.e., the AQ I/ORG interface, under constant inflow. Consequently a respective outflow of the same rate of B, CTA^+ , PH, $CTA-P$, and B' (*n*-butanol transferred to ORG) was taken into account. No flow conditions were imposed on species that are adsorbed at the interface, such as CTA^+-I , $P^- - I$, $B - I$, and I itself. Note that in this respect the interface is treated as the reactor.

The corresponding model reactions M1–M5 and their rates (R) as well as the respective differential equations used for our simulations are given in Table 1.

Figure 5 shows the result of a numerical simulation of the model after respective flow terms for the nonadsorbed species have been included. Oscillations were observed for $P^- - I$ and I , as shown, as well as for all other species including H^+ . The oscillations in $[H^+]$ qualitatively reproduce the oscillatory behavior in pH close to the liquid–liquid interface, as has been observed in earlier experiments.^{3a,g}

The kinetic parameters k_1 – k_5 , the flow rate constant k_f , and the concentrations of the entering species $[B]_0$, $[CTA^+]_0$, and $[P^-]_0$ have been chosen arbitrary. At the beginning of the simulation, all variables were set to zero except of $[I]_0 = 1.0 \text{ M}$.

The shape of the oscillations in $P^- - I$ shows similarities to those that have been experimentally observed (Figure 1).

The model neither provides an explanation for the apparent occurrence of mixed-mode oscillations in the experiment nor for the observed interfacial movements at the beginning of the U-tube experiment. As mentioned, we did not find a correlation between the periodic macroscopic movements and the spike-shaped oscillations in the electrical potential of significantly lower frequency. However, the second oscillation pattern that we observed shows similarities in the frequency to that of the hydrodynamic movements. Thus, we consider the existence of two independent oscillatory pathways in the system: one of chemical origin related to periodic interfacial processes as tentatively described by our model and the other of hydrodynamic nature which is still to be understood and which is not included into the model scheme. Our assumption of different oscillatory pathways has been recently supported by Shioi et al.²¹ The authors found for a similar system that thermal flow or the Marangoni effect cannot be at the origin of the spike-pattern oscillations such as we observed in our experiments. Using a theoretical model, the above authors obtained regular

oscillations of the interfacial tension, but when they added a term for the Marangoni flow to their equations, they obtained a pattern of noisier and less regular oscillations that were similar to the small oscillations that we observed experimentally.

Conclusion

In this paper, we revisited the oscillatory picric acid/CTAB two-phase in the U-tube reactor. New experimental results clarified the role of some key processes and compounds that have been subject of speculations since the system was first reported by Dupeyrat and Nakache.^{5,6} In particular, we confirmed that oscillations occur at the interface between CTAB/alcohol in water and picric acid in the organic solvent. We also showed that the formation of 1:1 ion pairs and not of reverse micelles is the key process by which CTA^+ coming from the aqueous phase and picrate coming from the organic phase interact to yield $CTA-P$.

A first experimentally supported explanation was given for the nonlinear behavior on the basis of our findings that the presence of the alcohol, which was shown to be essential to observe oscillatory behavior in the U-tube experiment, which inhibits the formation of the $CTA-P$ ion pairs. This inhibition became stronger the higher the concentration of the initial alcohol was. We also observed by S-shaped kinetic curves that the inhibition was released in the course of the process by apparently the removal of the inhibitor.

We proposed a kinetic mechanism for the nonlinear dynamics that is based on Langmuir–Hinshelwood adsorption kinetics. Thus, we assumed that the key dynamics occur exclusively at the aqueous/organic interface that was considered to remain constant in size throughout the experiment. We also assumed that the adsorbing species (CTA^+ , B, and picrate) compete for a limited and a constant total number of sites at the interface. The inhibition by the alcohol and its release cause nonlinear dynamics that are amplified by the autocatalytic step (M5). This leads to oscillatory behavior under flow conditions. The inhibition–acceleration dynamics were expressed by the adsorption of the alcohol at the interface, resulting in the inhibition of $CTA-P$ formation. In a second process, the adsorbed alcohol can autocatalytically detach from the interface and move into the organic phase—consequently, the inhibition is released by the removal of the inhibitor. The essential feedback is given by the assumption that the rates of the two processes are cross-linked and controlled by the amount of free interface that is available.

As a translation of the proposed mechanism we compiled a kinetic model. Instead of using diffusive fluxes, which control the experimental system, we treated the model system as a continuous flow reactor in which a constant flow of reactants was directed to the aqueous/organic interface (that is the reactor) and a respective outflow of products from the interface was taking place. Our simulations confirmed in a qualitative way that the proposed mechanism, in which the release of inhibition plays the key role, can indeed lead to oscillatory dynamics.

We are aware that the simplified treatment in the framework of the present kinetic mechanism does not take into account entirely the possible importance of competing diffusive fluxes. Further studies are planned to clarify this point and to obtain a more quantitative kinetic model of the system.

Acknowledgment. The authors wish to thank Dominique Lavabre (Université Paul Sabatier, Toulouse, France) for providing and helping us with the Sa 2.0 program that was used

for the computer simulations and Caroline Roque for near-infrared measurements.

References and Notes

- (1) (a) Bachmann, P. A.; Luisi, P. L.; Lang, J. *Nature* **1992**, *357*, 57–59. (b) Buhse, T.; Nagarajan, R.; Lavabre, D.; Micheau, J. C. *J. Phys. Chem. A* **1997**, *101*, 3910–3917. (c) Buhse, T.; Lavabre, D.; Nagarajan, R.; Micheau, J. C. *J. Phys. Chem. A* **1998**, *102*, 10552–10559. (d) Tixier, J.; Pimienta, V.; Buhse, T.; Lavabre, D.; Nagarajan, R.; Micheau, J. C. *Colloids Surf., A* **2000**, *167*, 131–142.
- (2) Buhse, T.; Pimienta, V.; Lavabre, D.; Micheau, J. C. *J. Phys. Chem. A* **1997**, *101*, 5215–5217.
- (3) (a) Yoshikawa, K.; Matsubara, Y. *J. Am. Chem. Soc.* **1983**, *105*, 5967–5969. (b) Nakata, S.; Ukitsu, M.; Yoshikawa, K. In *Proceedings of the International Conference on Dynamical Systems and Chaos*; Aoki, N., Shiraiwa, K., Takahashi, Y., Eds.; World Scientific: Hong Kong, 1994; Vol. 1, pp 339–342. (c) Yoshihisa, H.; Miyamura, K.; Gohshi, Y. *Chem. Lett.* **1997**, 1031–1032. (d) Sutou, S.; Yoshihisa, H.; Miyamura, K.; Gohshi, Y. *J. Colloid Interface Sci.* **1997**, *187*, 544–546. (e) Maeda, K.; Hygogo, W.; Nagami, S.; Kihara, S. *Bull. Chem. Soc. Jpn.* **1997**, *70*, 1505–1507. (f) Yoshidome, T.; Higashi, T.; Mitsushio, M.; Kamata, S. *Chem. Lett.* **1998**, 855–856. (g) Toko, K.; Yoshikawa, K.; Tsukiji, M.; Nosaka, M.; Yamafuji, K. *Biophys. Chem.* **1985**, *22*, 151–158.
- (4) (a) Yamaguchi, T.; Shinbo, T. *Chem. Lett.* **1989**, 935–938. (b) Kai, S.; Müller, S. C.; Mori, T.; Miki, M. *Phys. D* **1991**, *50*, 412–428. (c) Yoshikawa, K.; Magome, N. *Bull. Chem. Soc. Jpn.* **1993**, *66*, 3352–3357. (d) Magome, N.; Yoshikawa, K. *J. Phys. Chem.* **1996**, *100*, 19102–19105.
- (5) Dupeyrat, M.; Nakache, E. *Bioelectrochem. Bioenerg.* **1978**, *5*, 134–141.
- (6) Dupeyrat, M.; Nakache, E. In *Synergetics Far from Equilibrium*; Pacault, A., Vidal, C., Eds.; Springer-Verlag: Berlin, 1979; pp 156–160.
- (7) (a) Sterling, C. V.; Scriven, L. E. *AIChE. J.* **1959**, *5*, 514–523. (b) Scriven, L. E.; Sterling, C. V. *Nature* **1960**, *187*, 186–188.
- (8) (a) Yoshikawa, K.; Matsubara, Y. *Biophys. Chem.* **1983**, *17*, 183–85. (b) Yoshikawa, K.; Matsubara, Y. *J. Am. Chem. Soc.* **1984**, *106*, 4423–4427.
- (9) Takahashi, S.; Tsuyumoto, I.; Kitamori, T.; Sawada, T. *Electrochim. Acta* **1998**, *44*, 165–169.
- (10) Sa (Simulation + adjustment) is a noncommercial program based on C²⁺ that was developed at the Laboratoire de IMRCP, Université Paul Sabatier, Toulouse, France.
- (11) Kaps, K.; Rentrop, P. *Comput. Chem. Eng.* **1984**, *8*, 393.
- (12) In contrast to previous studies (refs 3a, 5, 6, and 8), we used CH₂Cl₂ instead of nitrobenzene or nitromethane as the organic solvent because of its virtual transparency in the region of $\lambda = 300$ –500 nm.
- (13) Arai, K.; Kusu, F.; Takamura, K. *Chem. Lett.* **1990**, 1517–1520.
- (14) Pramauro, E.; Pelezetti, E. In *Comprehensive Analytical Chemistry*; S. G. Weber, Ed.; Elsevier: Amsterdam, 1996; Vol. XXXI, p 12.
- (15) Job, F. *Ann. Chim.* **1928**, *9*, 113–202.
- (16) Observations and the recording of the Job diagram refer to equilibrium properties of the system. At the beginning of each experiment for various χ , we always observed a plane meniscus between the aqueous and organic phase.
- (17) Bruneau, E.; Lavabre, D.; Levy, G.; Micheau, J. C. *J. Chem. Educ.* **1992**, *69*, 833–837.
- (18) Giustini, M.; Palazzo, G.; Colafemmina, G.; Monica, M. D.; Giomini, M.; Ceglie, A. *J. Phys. Chem.* **1996**, *100*, 3190–3198.
- (19) (a) Seno, M.; Araki, K.; Shiraiishi, S. *Bull. Chem. Soc. Jpn.* **1976**, *49*, 899–903. (b) Sunamoto, J.; Hamada, T.; Seto, T.; Yamamoto, S. *Bull. Chem. Soc. Jpn.* **1980**, *53*, 583–89. (c) Seno, M.; Sawada, K.; Araki, K.; Iwamoto, K.; Kise, H. *J. Colloid Interface Sci.* **1980**, *78*, 57–64.
- (20) Miranda, P. B.; Pflumio, V.; Saijo, H.; Shen, Y. R. *J. Am. Chem. Soc.* **1998**, *120*, 12092–12099.
- (21) Shioi, A.; Sugiura, Y.; Nagoaka, R. *Langmuir* **2000**, *16*, 8383–8389.